A Solar Cell Photo-Luminescence Modulator for Optical Communications

Walter D. Leon-Salas *Member, IEEE*, Xiaozhe Fan, Miguel Vizcardo and Mauricio Postigo-Malaga

***Abstract*—This paper presents a circuit suitable for the modulation of the photo-luminescent radiation of a solar cell. The circuit uses a MOSFET and a low-power amplifier in a feedback loop and acts as a variable load to the solar cell. By controlling the current drawn from the solar cell, the proposed circuit is able to set the solar cell's voltage to any value between 0 V and the open circuit voltage. A circuit analysis of the modulator is presented along with experimental validation. As a proof of concept, a hardware prototype was built to demonstrate an optical communication link with the proposed modulator and a GaAs solar cell. Measurement results show that a bit error rate of 3.54×10^{-4} can be achieved at a rate of 40 kbps and at a distance of 30 cm.**

***Index Terms*—optical communications, solar cells, photo-luminescence, modulation.**

I. Introduction

THE use of solar cells as photo-receptors in receivers for visible light communications has been explored before [1]–[12]. The motivation for this approach is that by using a solar cell for two purposes, namely to harvest ambient radiant energy and to receive data wirelessly, savings in costs and space will be achieved, which would be advantageous for Internet-of-Things (IoT) applications. This approach was further extended in [13,14] to use GaAs solar cells as light emitters for data *transmission*. In this technique, dubbed Optical Frequency Identification (OFID), the electro-luminescent (EL) and photo-luminescent (PL) radiation of GaAs solar cells is modulated to transmit information wirelessly. Due to their direct bandgap electronic structure, GaAs solar cells have strong EL and PL emissions in the near infrared (NIR), peaking around 860 nm, which can be detected using a Si photo-diode or a CMOS camera. In order to modulate the luminescence of a solar cell, it is necessary to vary the voltage across its terminals because the luminescent optical power emitted by a solar cell is a function of its voltage [16].

The basic PL modulator is a MOSFET that works as a switch to short the terminals of the solar cell or leave them in open circuit (OC), thus, setting the cell's voltage to either 0 V or to the OC voltage (V_{oc}) [13,15]. While simple to implement, this type of on-off modulator fully discharges the solar cell's internal capacitance while it is being shorted. This capacitance needs to be re-charged before the next symbol can be transmitted. The time to re-charge this internal capacitance is a function of the luminous flux falling on the solar cell and the area of the solar cell. An improved PL modulator that exploits the relationship between the input impedance of a boost DC-DC converter and the duty cycle of its clock input is described in [14] and was employed to change the voltage across the solar cell and modulate the solar cell's PL. This approach allows the existence of modulation levels between short and OC voltages, thus, it is possible to use it with M-ary modulation and also to avoid fully shorting the solar cell. However, due to the large input capacitance of a boost DC-DC converter, the modulation speed of this modulator is limited to few kilobits per second (kbps). Moreover, the switching action of the DC-DC converter introduces ripple noise, which would be of concern for M-ary modulation.

This paper presents a circuit suitable for the modulation of the PL radiation of GaAs solar cells. The circuit uses a MOSFET and a low-power operational amplifier (opamp) in a feedback loop and works as a variable load to the solar cell. By controlling the current drawn from the solar cell, the proposed modulator is able to set the solar cell's voltage to a target value between 0 V and V_{oc}. This circuit allows M-ary modulation and does not require a full discharge of the solar cell's internal capacitance. Hence, it can achieve higher speeds than an on-off modulator. Moreover, it does not introduce ripple noise.

II. Photo-Luminescence in Solar Cells

The PL radiation emitted by a solar cell is the product of radiative recombination of electron-hole pairs generated inside the solar cell when the cell is illuminated. For GaAs, which has a bandgap energy of 1.42 eV, the emitted photons are in the near infrared (NIR) band (peaking at wavelength of approximately 873 nm). For an ideal solar cell (without losses), the emitted PL radiation should exactly balance the incoming light. A counter-intuitive result discussed in [17] states that efficient external luminescence is a necessary condition for approaching the Shockley-Queisser limit. Thus, a good solar cell also needs to be designed to be a good light emitting diode (LED).

If the solar cell is kept in OC, energetic electrons in the conduction band must remain inside the cell. Eventually most of these electrons recombine radiatively emitting photons. Thus, in OC the radiated PL is at its maximum and, for efficient GaAs solar cells, it can be readily detected with a CMOS camera. If a short circuit (SC) is applied to the solar

This work was supported by the National Science Foundation through award ECCS-1809637 and by the Universidad Nacional de San Agustin de Arequipa, Peru. *(Corresponding author: Walter D. Leon-Salas.)*

Walter D. Leon-Salas is with the School of Engineering Technology, Purdue University, Indiana 47907, United States (e-mail: wleonsal@purdue.edu). Xiaozhe Fan was with the School of Engineering Technology, Purdue University. He is now with Globalfoundries, Burlington, United States. Miguel Vizcardo is with the Physics Department, Universidad Nacional de San Agustin de Arequipa, Peru. Mauricio Postigo-Malaga is with the Department of Electronic Engineering, Universidad Nacional de San Agustin de Arequipa, Peru.

cell, the majority of the electrons inside the cell leave and flow through the external circuit. In this case, the PL radiated by the solar cell is greatly reduced since only a small fraction of the photo-generated electrons remain in the solar cell and are available for radiative recombination.

The experimental setup depicted in Fig. 1(a) was built to characterize the PL radiated by a solar cell. A GaAs solar cell from Alta Devices was employed in this work. These solar cells have a record efficiency of 29% [18] achieved with the help of a reflective back contact, which enhances photon recycling. A high-power LED with an spectrum peaking at 625 nm was used to illuminate the solar cell in order to stimulate a PL response. The solar cell was illuminated with an irradiance of 1.99 μW/cm^2. The PL irradiance, E_{pl}, was measured using an optical power sensor at a distance of 30 cm from the solar cell as the voltage across the solar cell was varied from 0 V to the OC voltage ($V_{oc} = 0.964$ V). The voltage across the solar cell was varied in discrete increments using a source meter. A long pass optical filter with a cutoff wavelength of 800 nm was placed in front of the optical power sensor to block light from the LED. In order to obtain repeatable results, this setup was placed inside an enclosure to block ambient light.

Using the reciprocity relation, it can be shown that the luminescent optical power emitted by the solar cell is an exponential function of the voltage across the solar cell V_D [16]. Hence, E_{pl}, can be modeled as follows:

$$E_{pl} = E_o + E_s\left(e^{V_D/nV_T} - 1\right) \quad (1)$$

where, E_o, E_s and n are model parameters. In particular, E_o is the SC irradiance, n is an ideality factor and V_T is the thermal voltage. The values of the model parameters can be estimated

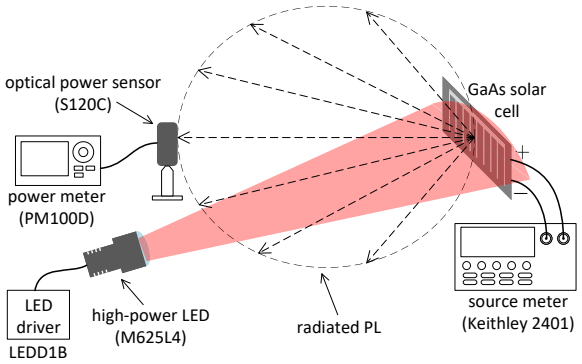

(a)

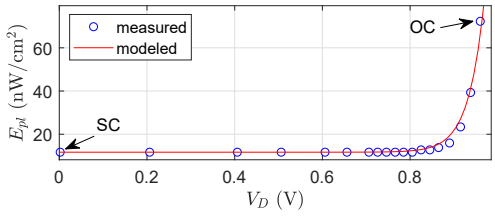

(b)

Fig. 1. Characterization of PL irradiance from a GaAs solar cell. (a) block diagram of the experimental setup; (b) measured and modeled irradiance. The SC and OC points are marked.

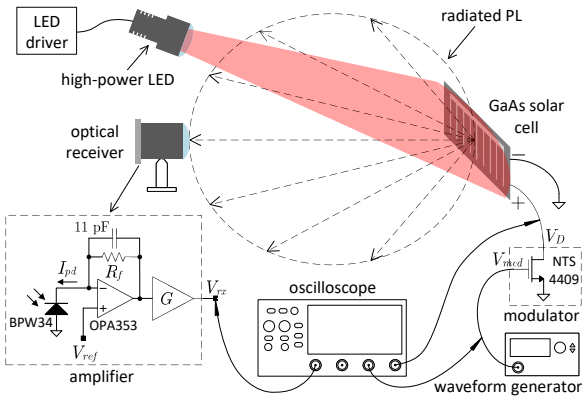

Fig. 2. Block diagram of experimental setup built to characterize the modulation speed of the on-off modulator.

by curve fitting (1) to measured data. Fig. 1(b) shows the measured and modeled irradiance. The values of the estimated model parameters are: $E_0 = 1.17\times10^{-8}$ W/cm^2, $E_s = 2.90\times10^{-19}$ W/cm^2 and $n = 1.375$. In the figure, the SC and OC points are marked. Notably, the PL irradiance is an exponential function of the voltage across the solar cell V_D.

This result shows that in order to modulate the emitted PL irradiance, one must vary V_D. The most basic modulator is an on-off modulator implemented using a switch. The switch used to short the terminals of the solar cell ($V_D = 0$ V) or leave them in OC ($V_D = V_{oc}$). Although simple, the drawback of this modulator is that, during SC, it fully discharges the solar cell's internal capacitance. Recharging this capacitance takes some time and results in a delayed PL response, which ultimately limits the maximum modulation rate.

To characterize the charging time of the solar cell's internal capacitance, the setup shown in Fig. 2 was built. The solar cell was illuminated using the same conditions employed in the characterization shown in Fig. 1. An optical receiver was placed in front of the solar cell at a distance of 30 cm and the on-off modulator was implemented using a MOSFET to periodically short the terminals of the solar cell. The optical receiver comprised a focusing lens, a photo-diode and an amplifier.

Fig. 3 shows the modulator input waveform, V_{mod}, along with the voltage across the solar cell, V_D, and the output of receiver V_{rx}. When V_{mod} is high, the MOSFET turns on and shorts the terminals of the solar cell, as a consequence V_D collapses to 0 V. When V_{mod} is low, the MOSFET turns off and V_D raises up to V_{oc} as the solar cell's internal capacitance gets re-charged by the cell's photo-generated current. It can be seen that it takes about 0.1 ms for this re-charging to complete (under the conditions stated above). Moreover, due to the exponential relationship between E_{pl} and V_D, V_{rx} does not change appreciably until V_D is sufficiently close to V_{oc}. This results in an apparent delay between V_{mod} and V_{rx} (shown as Δt in the figure), which precludes the maximum transmission speed that can be achieved with the on-off modulator to about 5 kbps (when pulse position modulation is used).

To gain insight into the limiting factors of the on-off modulator, a circuit analysis was performed. For this analysis, the equivalent circuit for the solar cell shown in Fig. 4 was

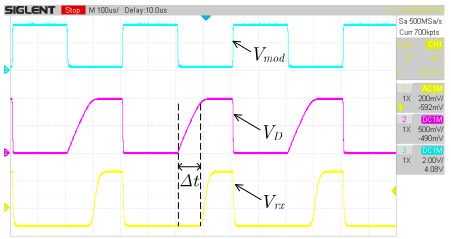

Fig. 3. Acquired waveforms when an on-off modulator is used. V_{mod} drives the MOSFET's gate, V_D is the voltage across the solar cell and V_{rx} is the optical receiver's output.

employed. In this equivalent circuit, I_{ph} is the photo-generated current, R_{sh} is the shunt resistance that models the load presented to the current generated near the edges of the solar cell, C_j is the junction capacitance and R_{sr} is the series resistance due to device contacts and connections [19]. The diode models the behaviour of the solar cell's pn junction. In our case, this diode is also an LED responsible for the NIR luminescent radiation. The current through this diode is given by Shockley's equation: $I_d = I_s(e^{V_d/nVT} - 1)$, where I_s is the solar cell's reverse saturation current.

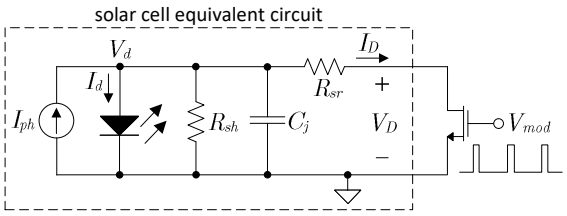

Fig. 4. Equivalent circuit employed for the analysis of an on-off PL modulator.

Using the circuit in Fig. 4 and considering that $R_{sr} \approx 0$, which results in $V_d \approx V_D$, the differential equation in (2) was derived and solved using numerical methods.

$$\frac{dV_D}{dt} = \frac{I_{ph} + I_s}{C_j} - \frac{I_s}{C_j} e^{V_D/nV_T} - \frac{1}{R_{sh}C_j} V_D. \qquad (2)$$

Fig. 5 shows the measured waveform and the numerical solution for the solar cell's voltage for an initial condition of $V_D = 0$ V (SC) and for $I_{ph} = 8.2$ mA, $R_{sh} = 6.57$ kΩ and $C_j = 700$ nF. These parameters were estimated using the methods described in [20] and [21]. Notably, V_D increases steadily, as the internal junction capacitance charges up, until it reaches the OC voltage ($V_{oc} = 0.964$ V).

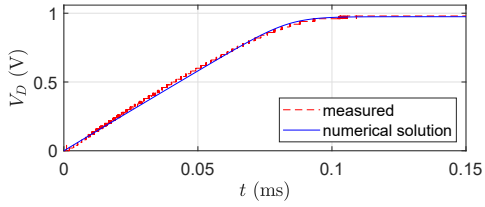

Fig. 5. Measured and calculated voltage across the solar cell, V_D, after it has been short circuited.

The output of the receiver's amplifier, V_{rx}, is a linear function of the photo-current I_{ph} and can be calculated as follows:

$$V_{rx} = I_{ph} \times R_f \times G \qquad (3)$$

where, R_f is the feedback resistor and G is the gain of the second stage of the amplifier. Moreover, $I_{ph} = P_{rx}R_\lambda$, where P_{rx} is power received by the optical receiver and R_λ is responsivity of the receiver's photo-diode. P_{rx} can be estimated from the irradiance using:

$$P_{rx} = A_{lens} \times E_{pl} \qquad (4)$$

where, A_{lens} is the area of the receiver's lens. Combining the solution of (2) with (1), (3) and (4), the receiver's output V_{rx} was estimated and is shown in Fig 6 (for $R_f = 100$ kΩ, $G = 10$, $A_{lens} = 5.07$ cm^2 and $R_\lambda = 0.68$ A/W). This result matches well with the acquired waveforms shown in Fig. 3 and it also shows that V_{rx} starts to rise only after V_D has risen above 0.835 V or about 86% of V_{oc}. This delayed response in V_{rx} is due to the non-linear and exponential relationship between the emitted PL and V_D. It also suggests that an improved PL modulator does not need to fully short circuit the solar cell to significantly change the solar cell's PL.

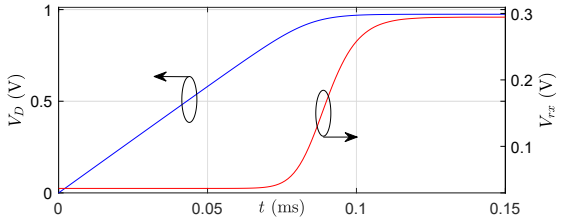

Fig. 6. Voltage across the solar cell, V_D, and output voltage of optical receiver, V_{rx}, as the solar cell's internal capacitance charges up from SC.

III. Proposed Modulator

Fig. 7 depicts the proposed PL modulator circuit. This circuit is able to set the voltage across the solar cell to any value between 0 V and V_{oc} using the feedback loop formed by a MOSET (M_1) and an opamp (A_1) connected as shown in the figure. The figure also shows how the modulator gets connected to a DC-DC converter. When EH is high (energy harvesting mode), the switch S_1 closes and the solar cell gets connected to the DC-DC converter allowing power to be drawn from the solar cell and get transferred to a load. Moreover, during energy harvesting mode, S_2 connects the negative input terminal of the opamp (V_-) to V_{EH}, which is a voltage greater than V_{oc}. This causes the opamp's output to drop to 0 V turning off M_1. With M_1 off, all of the solar cell's output current flows into the DC-DC converter and maximum power from the solar cell can be harvested. V_{EH} can be connected to the output of a boost DC-DC converter.

When the signal EH is low (modulation mode), S_1 opens disconnecting the modulator from the DC-DC converter while V_- gets connected to the modulation input V_{mod}. The feedback loop sets M_1's gate voltage to a value that causes M_1 to draw just enough current from the solar cell to get V_D to drop from V_{oc} to the desired voltage V_{mod}. In this manner, M_1

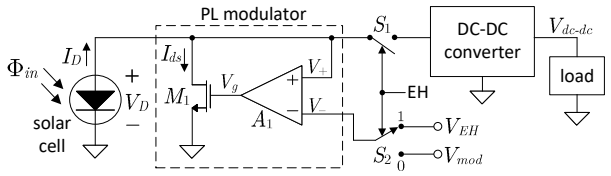

Fig. 7. Schematic diagram of the proposed PL modulator.

effectively appears as a variable load to the solar cell. Since in this mode the modulator is fully disconnected from the DC-DC converter, switching noise from the DC-DC converter does not affect modulation. However, energy cannot be harvested during this mode. Thus, this modulator is suitable for burst transmission. In order to verify the operation of this feedback loop, the equivalent circuits of the modulator and the solar cell shown in Fig. 8 were used to analyze the modulator.

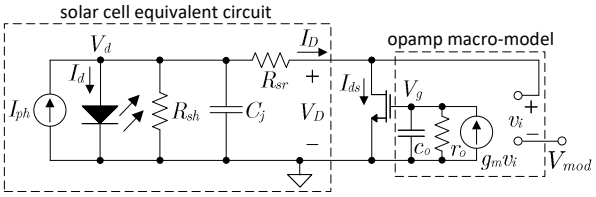

Fig. 8. Equivalent circuits of the solar cell and the proposed modulator employed to analyze the modulator's operation.

The following equations were derived from this circuit:

$$\begin{aligned} \frac{dV_g}{dt} &= \frac{A_o}{r_o c_o}(V_D - V_{mod}) - \frac{1}{r_o c_o} V_g \\ \frac{dV_D}{dt} &= \frac{I_{ph} + I_s}{C_j} - \frac{I_s}{C_j} e^{V_D/nV_T} - \frac{1}{R_{sh} C_j} V_D - \frac{I_{ds}}{C_j} \end{aligned} \quad (5)$$

where, $r_o c_o = A_o/(2\pi \times GB)$, $g_m = A_o/r_o$, A_o is the opamp's DC gain and GB is its gain-bandwidth product. Three regions of operation for M_1 were considered (sub-threshold, saturation and triode). Thus, I_{ds} was modeled as follows:

$$I_{ds} = \begin{cases} I_o \frac{W}{L} e^{(V_g - V_{TH})/nV_T} & \text{if } V_g < V_{TH} \\ \frac{\beta}{2}\left(V_g - V_{TH}\right)^2 & \text{if } V_D \geq V_g - V_{TH} \\ \beta\left((V_g - V_{TH})V_D - \frac{V_D^2}{2}\right) & \text{if } V_D < V_g - V_{TH} \end{cases} \quad (6)$$

where, V_{TH} is the threshold voltage of the transistor, W/L its width-length ratio and β its transconductance. The (5)-6) set of equations was solved numerically. Fig. 9 shows the solution for V_D as V_{mod} increases linearly for the following parameter values: $V_{TH} = 0.85$ V, $GB = 500$ kHz, $A_o = 90$ dB, $\beta = 0.48$ S, $W/L = 10,000$ and $I_o = 10$ nA. Notably, V_D follows V_{mod} until it reaches V_{oc}. As V_{mod} increases beyond V_{oc}, V_g goes to 0 V and M_1 is turned off, leaving the solar cell in OC.

The functionality of the modulator was also verified experimentally using the test setup shown in Fig. 2 in which the on-off modulator was replaced with the proposed modulator. The proposed modulator was implemented using the NTS4409 MOSFET and the low-power TLV2761 opamp, which has a supply current consumption of 20 μA [22].

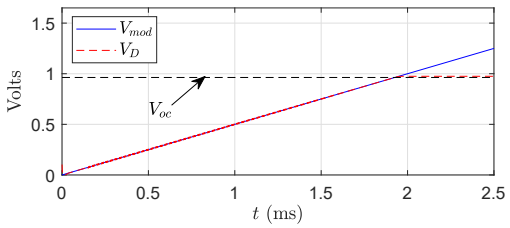

Fig. 9. Numerical solution of the proposed modulator circuit. V_D follows the modulation input V_{mod} until it reaches V_{oc}.

Due to this exponential relationship, the receiver's output, V_{rx}, does not rise until V_D is sufficiently high (as shown in Fig. 6). To establish the modulation amplitude that results in the fastest response for binary pulse modulation, the following experiment was carried out: V_D was modulated with a square pulse, with a voltage excursion from V_{low} to V_{oc}, and the receiver output V_{rx} was recorded. Fig. 10 shows the results of this experiment for different values of V_{low}. It can be seen that as V_{low} decreases, it takes longer for V_{rx} to start rising. On the other hand, if V_{low} is too high, i.e. 0.95 V_{oc}, the output pulse's amplitude decreases. A good compromise is to set V_{low} to 0.85 V_{oc} or 0.90 V_{oc}. In practice, V_{oc} is measured periodically as part of most maximum power point tracking algorithms.

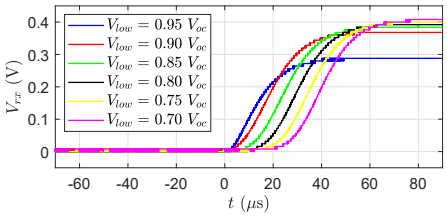

Fig. 10. Acquired waveforms at the output of the optical receiver as V_D is modulated with a square pulse with voltage excursion from V_{low} to V_{oc}.

As a test, the solar cell's luminescence was modulated with a random sequence of bits to asses the performance of a PL-based optical communication link using the proposed modulator. For this test, a binary differential pulse interval modulation (DPIM) scheme was employed as it has been shown to be advantageous for optical communications [23]. In this scheme, the 0 symbol was represented by a pulse of width T_p followed by a quite period of T_0 seconds while the 1 symbol was represented by a pulse of width T_p followed by a quite period of T_1 seconds. For this test the proposed modulator circuit was employed with the test setup of Fig. 2. Fig. 11 shows waveforms acquired from the modulator as bits were transmitted for $V_{low} = 0.90 \times V_{oc}$, $T_p = 10$ μs, $T_0 = 15$ μs and $T_1 = 40$ μs. A measured bit error rate (BER) of 7.71×10^{-6} for 388,874 transmitted bits was obtained at a rate of 26.67 kbps.

Another test was performed to demonstrate the capability for multi-level (M-ary) modulation of the proposed circuit. Due to the non-linear relationship between E_{pl} and V_D, the modulator's input voltage levels (V_{mod}) have to be non-equally spaced in order to achieve equally-spaced levels at the receiver's output (V_{rx}). This voltage level mapping can be calculated using (1), (3) and (4). Fig. 12 shows acquired waveforms for 4 modulation levels. A BER of 3.54×10^{-4} was

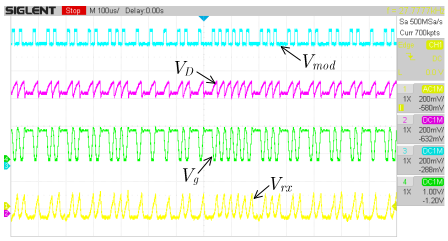

Fig. 11. Acquired waveforms from a PL-based optical communication system that uses the proposed modulator circuit.

achieved using 4-ary modulation and a symbol duration of 50 μs, equivalent to a communication speed of 40 kbps.

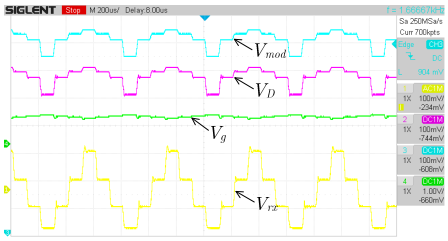

Fig. 12. Acquired waveforms showing multi-level modulation.

Finally, Table I compares the performance of the proposed circuit with other PL modulators in terms of speed, hardware complexity, energy harvesting capability, ripple noise and support for M-ary modulation.

TABLE I
PERFORMANCE COMPARISON OF PL MODULATORS

reference	speed (kbps)	hardware complexity	energy harvesting	ripple noise	M-ary capable
[14]	10	MOSFET, mux DC-DC conv.	yes	yes	yes
[15]	15	AND gate, MOSFET, DC-DC conv.	yes	yes	no
[24]	1.2	MOSFET, DC-DC conv.	yes	yes	no
this work	40	MOSFET, opamp	no	no	yes

IV. Conclusion

This paper has presented a circuit comprising a MOSFET and a low-power opamp in a feedback loop which can be used to modulate the photo-luminescence of a solar cell. Unlike other alternatives, the proposed modulator does not introduce switching noise and it does not fully discharge the solar cell's internal capacitance, which enables it to achieve higher speeds than an on-off modulator. The proposed modulator can be used in energy harvesting devices to allow them to re-use their on-board solar cells to transmit information optically. A circuit analysis of the modulator was presented along with experimental validation. A proof-of-concept prototype was used to demonstrate an optical communication link using a GaAs solar cell as the transmitter. The proposed modulator is also suitable for full on-chip integration.

References

[1] J. Fakidis, M. Ijaz, S. Kucera, H. Claussen and H. Haas, "On the design of an optical wireless link for small cell backhaul communication and energy harvesting," *IEEE Annual International Symposium on Personal, Indoor and Mobile Radio Communication (PIMRC)*, Sept. 2014.

[2] Z. Wang, D. Tsonev, S. Videv and H. Haas, "Towards self-powered solar panel receiver for optical wireless communications," *IEEE International Conference on Communications (ICC)*, June 2014.

[3] Z. Wang, D. Tsonev, S. Videv and H. Haas, "On the design of a solar-panel receiver for optical wireless communications with simultaneous energy harvesting," *IEEE Journal on Selected Areas in Communications*, vol. 33, no. 8, pp. 1612-1623, 2015.

[4] H.-Y. Chen, K. Liang, C.-Y. Chen, S.-H. Chen, C.-W. Chow and C.-H. Yeh, "Passive optical receiver for visible light communication (VLC)," *IEEE Region 10 Conference TENCON*, Nov. 2015.

[5] S. Zhang, D. Tsonev, S. Videv, S. Ghosh, G. A. Turnbull, I. F. W. Samuel and H. Haas, "Organic solar cells as high-speed data detectors for visible light communications," *Optica*, vol. 2, no. 7, pp. 607-610, 2015.

[6] E. Bialic, L. Maret and D. Kténas, "Specific innovative semi-transparent solar cell for indoor and outdoor LiFi applications," *Applied Optics*, vol. 54, no. 27, pp. 8062-8069, 2015.

[7] J. Li, A. Lu, G. Shen, L. Li, C. Sun and F. Zhao, "Retro-VLC: enabling battery-free duplex visible light communication for mobile and IoT applications," *International Workshop on Mobile Computing Systems and Applications (HotMobile)*, pp. 21-26, Feb. 2015.

[8] S.-H. Lee, "A passive transponder for visible light identification using a solar cell," *IEEE Sensors Journal*, vol. 15, no. 10, pp. 5398-5403, 2015.

[9] B. Malik and X. Zhang, "Solar panel receiver system implementation for visible light communication," *IEEE International Conference of Electronics, Circuits and Systems (ICECS)*, Dec. 2015.

[10] R. Sarwar, B. Sun, M. Kong, T. Ali, C. Yu, B. Cong and J. Xu, "Visible light communication using a solar-panel receiver," *IEEE Int. Conf. on Optical Communications and Networks (ICOCN)*, Aug. 2017.

[11] X. Fan and W. D. Leon-Salas, "A circuit for simultaneous optical data reception and energy harvesting," *IEEE International Midwest Symposium on Circuits and Systems*, 2017.

[12] Y. Wang, P. Zhang, X. Wang, T. Wang D. Wang, L. Zhang and S Tong, "Spectrum effect on output characteristics of wireless energy and data hybrid transmission system using a solar panel," *International Conference on Information Optics and Photonics (CIOP)*, 2018.

[13] W. D. Leon-Salas and X. Fan, "Exploiting luminescence emissions of solar cells for Optical Frequency Identification (OFID)," *IEEE International Symposium on Circuits and Systems (ISCAS)*, May 2018.

[14] W. D. Leon-Salas and X. Fan, "Solar cell luminescence modulation for Optical Frequency Identification," *IEEE Trans. on Circuits and Systems*, vol. 66, no. 5, pp. 1981-1992, May 2019.

[15] W. D. Leon-Salas and X. Fan, "Photo-luminescence modulation circuits for solar cell based optical communications," *IEEE International Symposium on Circuits and Systems (ISCAS)*, pp. 1-5, 2019.

[16] U. Rau, "Superposition and reciprocity in the electroluminescence and photoluminescence of solar cells," *IEEE Journal of Photovoltaics*, vol. 2, no. 2, pp. 169-182, 2012.

[17] O. D. Miller, E. Yablonovitch and S. R. Kurtz, "Strong internal and external luminescence as solar cells approach the Schockley-Queisser limit," *IEEE Journal of Photovoltaics*, vol. 2, no. 3, pp. 303-311, 2012.

[18] M. Green, E. Dunlop, J. Hohl-Ebinger, M. Yoshita, N. Kopidakis, and X. Hao, "Solar cell efficiency tables (version 57)," *Progress in photovoltaics: research and applications*, vol. 29, no. 1, pp. 3-15, 2021.

[19] G. A. Rincon-Mora, "Harvesting microelectronic circuits," in *Energy Harvesting Technologies*, S. Priya and D. J. Inman, Eds. New York, NY, USA: Springer-Verlag, 2009.

[20] R. Kadri, H. Andrei, J.-P. Gaubert, T. Ivanovici, G. Champenois, and P. Andrei, "Modeling of the photovoltaic cell circuit parameters for optimum connection model and real-time emulator with partial shadow conditions," *Energy*, vol. 42, pp. 57–67, 2012.

[21] R. A. Kumar, M. S. Suresh and J. Nagaraju, "Time domain technique to measure solar cell capacitance," *Review of Scientific Instruments*, vol. 74, no. 7, pp. 3516-3519, 2003.

[22] Texas Instruments, 'TLV2761 single, 3.6-V, 500-kHz, RRIO operational amplifier'. [Online]. Available: https://www.ti.com/product/TLV2761. [Accessed: Dec. 8, 2021].

[23] Z. Ghassemlooy, A. R. Hayes, N. L. Seed, and E. D. Kaluarachchi, "Digital pulse interval modulation for optical communications," *IEEE Communications Magazine*, vol. 36, no. 12, pp. 95-99, 1998.

[24] X, Fan, S. Lee, W. D. Leon-Salas "An optical wireless temperature sensor," *IEEE Sensors*, 2019.